Vortex-dynamics approach to the Nernst effect in extreme type-II superconductors dominated by phase fluctuations

S. Raghu,[1] D. Podolsky,[2,3] A. Vishwanath,[2] and David A. Huse[4]
[1]*Department of Physics, Stanford University, Stanford, California 94305, USA*
[2]*Department of Physics, University of California, Berkeley, California 94720, USA*
[3]*Department of Physics, University of Toronto, Toronto, Ontario, Canada M5R 1A7*
[4]*Department of Physics, Princeton University, Princeton, New Jersey 08544, USA*
(Received 20 October 2008; published 26 November 2008)

We present a method to study the Nernst effect and diamagnetism of an extreme type-II superconductor dominated by phase fluctuations. We work directly with vortex variables and our method allows us to tune vortex parameters (e.g., core energy and number of vortex species). We find that diamagnetic response and transverse thermoelectric conductivity (α_{xy}) persist well above the Kosterlitz-Thouless transition temperature, and become more pronounced as the vortex core energy is increased. However, they *weaken* as the number of internal vortex states is increased. We find that α_{xy} closely tracks the magnetization ($-M/T$) over a wide range of parameters.

DOI: 10.1103/PhysRevB.78.184520 PACS number(s): 74.25.Fy, 74.20.De, 74.40.+k, 74.72.−h

A number of experimental observations in superfluidity and superconductivity are best explained in terms of the statistical mechanics and dynamics of vortices. Examples include the Kosterlitz-Thouless (KT) transition in superfluid films and the "flux-flow" contribution to electrical resistivity in type-II superconductors. A natural extension of this paradigm involves the use of thermoelectric and thermal transport experiments as a probe of vortex dynamics. This is especially pressing given the Nernst effect experiments in the cuprates.[1] The Nernst effect is the appearance of a steady-state electric field (E_y) when a system is placed in a perpendicular thermal gradient ($\nabla_x T$) and magnetic field (H^z) under open-circuit conditions. In the cuprate superconductors, a large Nernst signal and diamagnetism persists well above T_c, the superconducting transition temperature, and are especially enhanced in the underdoped regime of hole-doped materials.

To explain these results, it has been argued that vortices are responsible for the large Nernst signal:[1] as a vortex drifts down the temperature gradient, it generates a transverse electric field. A vortex description above T_c is useful when T_c marks the loss of macroscopic phase coherence, while the amplitude of the order parameter remains large below a higher "mean-field" temperature scale $T_c^{\mathrm{MF}} > T_c$.[2] This idea is most likely to hold true in the underdoped regime of the hole-doped cuprates, where the reduced superfluid stiffness enables phase fluctuations to suppress T_c below the mean-field transition temperature. Prior to the experiments described in Ref. 1, optical conductivity measurements[3] showed that superconducting correlations persist above T_c at short distance and time scales in BSCCO films. Recently, current-voltage measurements in YBCO films have also revealed a relatively wide zero-field regime where superconducting fluctuations are likely to persist.[4] However, the diamagnetism and Nernst measurements[1] have exposed a greater fluctuation regime since the normal state contributions to these experiments are far smaller than in electrical transport measurements. Over a range of fields, this "vortex-liquid regime" $T_c < T < T_c^{\mathrm{MF}}$ (Ref. 5) can be intuitively understood in terms of a dilute fluid of vortices, but so far this appealing picture[6,7] has not lead to a complete understanding of the Nernst effect.

There are special challenges involved in constructing a vortex-based theory of thermoelectric transport that is consistent with the basic principles of statistical mechanics. In contrast to thermodynamics, and even electrical transport, where a theory of vortices interacting via a long-range potential can be used, a thermal transport calculation requires a purely local formulation where no such long-range forces are explicitly present. In this paper, we present such a local formulation and use it to study thermoelectric transport directly in the vortex language. An advantage of our method is that vortex parameters, such as core energy or number of vortex species, can be tuned independently of other properties, and their impact on the Nernst signal and magnetization can be systematically studied. Moreover, it is possible to use our method to study the Coulomb gas efficiently even in the high-density limit, where the number of pairwise Coulomb interactions is large.

Previous theoretical work on the Nernst effect includes the time-dependent Ginzburg-Landau theory,[8,9] which includes fluctuations in the amplitude of the order parameter. The Nernst effect near a quantum critical point has been studied in Ref. 10. A heuristic treatment of the Nernst effect in a vortex liquid has been presented in Refs. 11. In earlier work, three of us have studied the Nernst effect in an *XY* model,[12] which should be relevant for the underdoped cuprates. Our present results approaching from the vortex viewpoint are consistent with this work. Remarkably, we find that the close quantitative connection between the Nernst effect and diamagnetism observed previously holds in the present study too, even when vortex properties are drastically modified. The effect of vortex core energy on thermodynamic properties was studied in Ref. 13.

Method: Consider a two-dimensional (2D) superconductor in the extreme type-II limit, in which the supercurrents are too feeble to modify the external field. We restrict the order parameter to live on the sites n of a square lattice

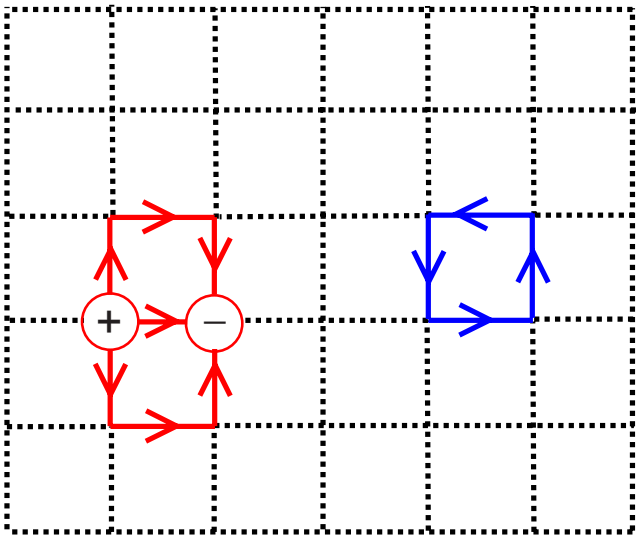

FIG. 1. (Color online) Charge updates (left) and curl updates (right) sample the longitudinal and transverse degrees of freedom, respectively, of the dual electric field.

and assume that all fluctuations arise from the phase: $\psi_n(t) = |\psi_0| e^{i\theta_n(t)}$. We map to the vortex representation by defining a *dual* electric field $\boldsymbol{e}=(e_i^x, e_i^y)$ on the bonds $(i, i+\hat{x})$ and $(i, i+\hat{y})$ of a dual lattice, orthogonal to the original lattice bonds, via $\boldsymbol{e}=\vec{\Delta}\theta\times\hat{z}$, where $\vec{\Delta}$ is a lattice derivative. Here the lattice spacing is taken to be the size of a vortex core. The local field $\boldsymbol{e}$ is related to the local supercurrents via $\boldsymbol{J}=\rho_s^0\hat{z}\times\boldsymbol{e}$, where ρ_s^0 is the bare superfluid density. Vortices may live at the sites i of this dual lattice, and the integer vortex charge n_i satisfies Gauss' law $\vec{\Delta}\cdot\boldsymbol{e}=2\pi n_i$. We then obtain a completely local Hamiltonian for the vortex fluid that retains all phase and vortex degrees of freedom,

$$\mathcal{H} = \frac{1}{4\pi}\sum_{i\in\text{links}} \boldsymbol{e}_i^2 + \epsilon_c \sum_{i\in\text{sites}} n_i^2, \tag{1}$$

where ϵ_c is the vortex core energy and we use units where $\rho_s^0 = 1/2\pi$. The dual electric fields can be decomposed into longitudinal and transverse components representing the vortex and supercurrent fluctuations, respectively. When the transverse electric fields are integrated out, the model reduces to the static 2D Coulomb gas. While the static Coulomb gas model is adequate for studying the equilibrium properties of a vortex fluid, we stress that one must include both local supercurrents and vortices when dealing with thermal transport so as to define a *local* energy density. The interaction between the vortices is mediated by the supercurrents, and this maps simply to the interaction between the charges being mediated by the dual electric field in our model.

The model is given a Monte Carlo dynamics that captures the effect of random thermal fluctuations. Two distinct types of Monte Carlo moves, electric curl and vortex updates, corresponding to the longitudinal and transverse degrees of freedom, are introduced (Fig. 1). During a curl update, a plaquette is chosen at random and a random electric curl is added to it. Such an update is purely transverse and is not accompanied by vortex creation. During a charge update, a lattice bond is chosen at random, and a vortex/antivortex pair is added on the two sites connected to this bond. The electric fluxes are updated locally near the charges to satisfy Gauss' law. The result of such an update is either the creation of a vortex/antivortex pair or the motion of a pre-existing vortex to a neighboring site. We note that while such moves can change the total number of vortices, the net vorticity does not change in a system with periodic boundary conditions. Each move is accepted with probability $1/[1+\exp(\Delta U/T)]$, where ΔU is the change in energy associated with the move and T is the local temperature at the center of the plaquette or bond for that move. By varying the relative frequency of each type of trial, we have control over D_{ph}, the phase diffusivity, relative to the vortex diffusivity D_v. In what follows, we work in the physically reasonable limit $D_{\text{ph}} \gg D_v$ (in practice we set $D_{\text{ph}}=25D_v$). After an attempt is made to update each bond and plaquette, a unit of Monte Carlo time elapses. A related method has been used in Ref. 14 to study charged polymers.

When a charge move is attempted, the simplest way to satisfy Gauss' law is to add an electric flux $\boldsymbol{e}=2\pi\hat{\boldsymbol{r}}$ to the link $\hat{\boldsymbol{r}}$ connecting the positive to the negative charge. However, such single bond updates are rarely accepted, resulting in too little vortex motion below a temperature scale $T\sim\pi/2\gg\rho_s^0$; to avoid this artificial vortex pinning, we use an update that spreads the electric flux over several bonds. A simple example of such an update is shown in Fig. 1. The added flux is made curl free, and the move we actually use involves a patch of 12 plaquettes that is one plaquette larger in all directions than indicated in Fig. 1. We have explicitly computed the vortex mobility from the voltage autocorrelation function and have seen its enhancement at lower temperatures with the use of such updates. As the size of the patch over which the updates are made is increased, the problems associated with fictitious vortex pinning are eliminated. However, when the charge updates are made over the entire system, the curl updates are no longer necessary as the excitations of the transverse component of the electric fields become instantaneous, making the model unsuitable for studying thermal transport. Therefore, the charge updates must be made over a region whose size is larger than the lattice spacing but much smaller than the entire system size. In our simulations, the charge updates are made over a region of 12 plaquettes that is one plaquette larger in all directions than indicated in Fig. 1. We have found that these moves eliminate the artificial pinning of vortices and allow us to access the dynamics down to T_{KT} but are still sufficiently local to permit the study of thermal transport.

Thermodynamics: We have studied the KT transition of the neutral 2D Coulomb gas by tracking the dielectric response function

$$\epsilon^{-1} = 1 - \frac{\left\langle \left(\sum_i \boldsymbol{e}_i\right)^2 \right\rangle}{4\pi T L^2}. \tag{2}$$

At $T=T_{\text{KT}}$, the dielectric response function satisfies the universal jump criterion[15]

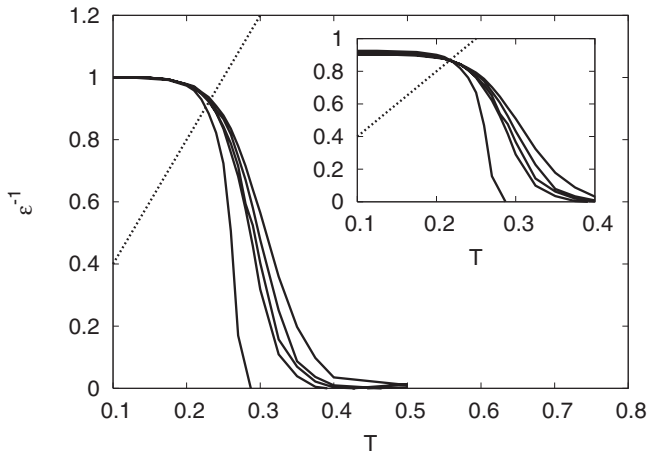

FIG. 2. Dielectric response of the dual Coulomb gas, computed using Eq. (2), and (inset) rescaled for finite-size effects (Ref. 16). We use an $L\times L$ torus with $L=8,10,12,14,40$ and core energy $\epsilon_c=0.125$. The transition temperature is the location where the rescaled data intersect the line $y=4T$ (dotted line).

$$\epsilon^{-1}=\begin{cases}4T_{\mathrm{KT}}, & T=T_{\mathrm{KT}}^{-}\\ 0, & T=T_{\mathrm{KT}}^{+}\end{cases}. \tag{3}$$

Figure 2 shows the results of the helicity modulus calculation using various system sizes and a core energy $\epsilon_c=0.125$. We use finite-size scaling[16] to identify $T_{\mathrm{KT}}=0.22$; the naive free-energy estimate is $T_{\mathrm{KT}}^0=0.25$ in our units. In the remainder of this paper, we cite all temperatures in units of T_{KT}^0.

Diamagnetism: When a magnetic field is applied, the resulting imbalance of vorticity leads us to consider a plasma of vortices in a static neutralizing background (charge density $n_b=-B/\Phi_0$, where $\Phi_0=2\pi$ is the flux quantum in our units). To study diamagnetism we permit vortices to enter and leave the sample by employing cylindrical geometry with open boundaries. Current flow near the boundaries is measured, which arises due to a surface depletion of vorticity that lowers the free energy relative to a perfectly neutral system. Deep inside the cylinder, beyond some distance x_0 from the edge, the supercurrents vanish in equilibrium. The magnetization can be obtained by inverting the relation $\boldsymbol{J}=\boldsymbol{\nabla}\times\boldsymbol{M}$ on a cylinder whose axis is along the x direction. For physical clarity we present continuum formulas below; these can be readily transcribed into the appropriate lattice versions,

$$M=\int_0^{x_0}dx\langle J^y(x,y)\rangle=\rho_s\int_0^{x_0}dx\langle e_x\rangle. \tag{4}$$

Thus, M is directly proportional to the *work function* of the dual Coulomb gas (energy cost of removing a vortex from the bulk of the system). Using Gauss' law we can also obtain

$$M=2\pi\rho_s\int_0^{x_0}dx\,x(\langle n(x)\rangle-B/\Phi_0). \tag{5}$$

Thus, M is also the total edge polarization per unit length. The polarization fields are nonzero only in the charge depletion region near the cylinder's edge.

Nernst effect: To determine the Nernst effect, we again make use of cylindrical geometry and apply a temperature gradient along the cylinder axis. We compute the transverse thermoelectric conductivity α_{xy} defined via $\langle J_y\rangle=-\alpha_{xy}(-\nabla_x T)$ and is closely related to the Nernst signal: α_{xy}/σ_{xx}. Here, σ_{xx} is the electrical conductivity and we have made the approximation of vanishing Hall angle. The expressions for the transport coefficients are easily found in the dual vortex representation using the relations

$$\boldsymbol{J}=\rho_s^0\hat{\boldsymbol{z}}\times\boldsymbol{e},$$

$$\boldsymbol{E}=\Phi_0\hat{\boldsymbol{z}}\times\boldsymbol{j}, \tag{6}$$

where upper (lower) case quantities refer to the original (dual) representation and $\boldsymbol{j}$ is the vortex current. The first equation above is the definition of the dual electric field, and the second is the Josephson relation. We observe that in the superconductor, the time-reversal operation, which maps $\boldsymbol{J}\to-\boldsymbol{J}$, translates to the particle-hole transformation, namely, $\boldsymbol{e}\to-\boldsymbol{e}$ in the dual vortex representation and vise versa. The quantity α_{xy} is obtained by measuring $\langle e^x\rangle$ and using the relation $\alpha_{xy}=\rho_s^0\langle e^x\rangle/\nabla_x T$. While α_{xy} is an *off-diagonal* transport coefficient when written in terms of electrical currents, it is a *diagonal* response function in the vortex representation: it is simply the vortex *thermopower*. We have verified that the net vortex motion vanishes once the steady state in the thermal gradient is reached, as is required in a thermopower measurement. The quantity α_{xy} has the advantage that, unlike the Nernst signal, it does not have any explicit dependence on Monte Carlo time t_{MC}, as can be seen from the Kubo formula for α_{xy} and dimensional analysis.[12] Also, in our model, the diagonal thermoelectric coefficient $\alpha_{xx}=\langle J_x\rangle/(-\nabla_x T)=\langle e^y\rangle/(\nabla_x T)$ maps onto a *transverse* thermopower of vortices. It vanishes by symmetry in our model since the vortices can travel perpendicular to the thermal gradient only if a Magnus force is present. However, a Magnus force can be nonzero only if particle-hole symmetry is broken in the superconductor (i.e., if the Hall angle is nonvanishing).

Figure 3 shows the simulation results for α_{xy} and M [inset (b)] for applied fields up to $B_0=\Phi_0/(2\pi a^2)$, where a is the lattice spacing, comparable to the zero-temperature coherence length ξ_0. Both α_{xy} and $-M/T$ are expressed in units of the 2D "quantum of thermoelectric conductance," $2ek_B/h$. We show data for $T\geq T_{\mathrm{KT}}^0$; below T_{KT}^0, our simulations encounter difficulties due to impaired vortex mobility. Fortunately, $T\geq T_{\mathrm{KT}}^0$ is a regime of interest since the Nernst signal persists well above T_c in the experiments of Wang, *et al.*[1] The results presented here are in quantitative agreement with earlier computations involving the 2D XY model with Langevin dynamics:[12] in particular, both models have the feature that in the small magnetic field limit, (a) α_{xy} and M diverge logarithmically as $B\to 0$ for $T\leq T_{\mathrm{KT}}$ and (b) they increase linearly with B at small B when $T>T_{\mathrm{KT}}$.[17] Moreover, both α_{xy} and M are detectable at temperatures as high as $2T_{\mathrm{KT}}$ in our model, as well as in the 2D XY model.[12] For $T\gg T_{\mathrm{KT}}$, the 2D XY model predicts that α_{xy} and M/T decay sharply as a power law in temperature. Here, the magnetization decreases even more rapidly at high temperatures: a calculation based

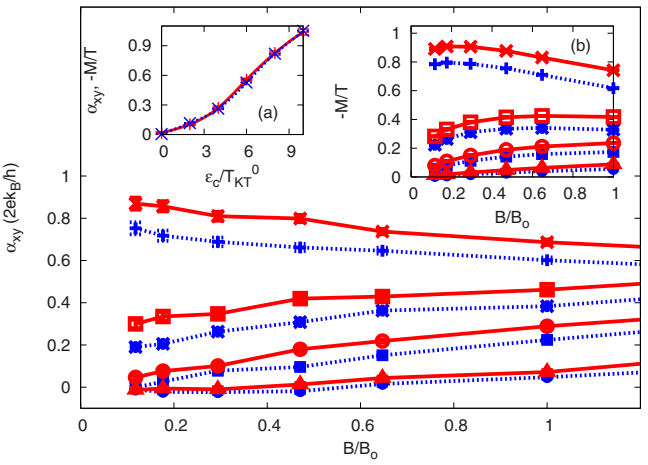

FIG. 3. (Color online) α_{xy} for a system of single-flavor (solid lines) and double-flavor (dotted lines) vortices on a 20×15 cylinder, with core energy $\epsilon_c=0.5T_{\mathrm{KT}}^0$. Temperatures shown are 1.0 (topmost 2 curves), 1.25, 1.5, and 2.0 T_{KT}^0 (bottom two curves). Inset (a): Core energy dependence of α_{xy} (solid lines) and $-M/T$ (dashed lines) in units of $2ek_B/h$ for single-flavor vortices, at $T=2.5T_{\mathrm{KT}}^0$ and $B=0.7B_0$, showing a marked increase in both quantities with core energy. Inset (b): Diamagnetism $-M/T$ curves for the same temperatures as the main figure. (Units of $2ek_B/h$ are used on the vertical axes of both insets.)

on the dual solid-on-solid model shows that the magnetization of single-flavor vortices decays exponentially as $M=-2T\sin(B/B_0)e^{-2T/\rho_s}$, and our numerical results agree with this expression. Although we have not succeeded in finding similar expressions for α_{xy}, our numerics indicate that α_{xy} also decays in this fashion at high temperatures and closely tracks $-M/T$.

Vortex core energy dependence: The core energy dependence of α_{xy} and $-M/T$ are shown in Fig. 3 [inset (a)] at $T=2.5T_{\mathrm{KT}}^0$. So long as $\epsilon_c \gtrsim T$, both are found to increase with ϵ_c. At this temperature, α_{xy} and $-M/T$ track each other closely. With increasing core energy, α_{xy} and $-M/T$ rise from near zero at $\epsilon_c=0$ to $O(1)$ at $\epsilon_c=10T_{\mathrm{KT}}^0$, showing that the core energy has a dramatic impact on both of these quantities in this regime. The dominant effect of ϵ_c is to enhance local superconducting correlations at short distances by increasing the cost of vortex fluctuations. It enters directly in setting the "work function" for removing a vortex from the system, which is proportional to the magnetization. For $\epsilon_c \gg T$, $-M \propto \epsilon_c$ since more vortices are expelled near the boundaries in this limit. We have observed this in our simulations. The vortex-free boundary layer grows with ϵ_c, and when it becomes comparable to the thickness of the sample this causes strong finite-size effects. Thus, we have not been able to reliably determine the bulk behavior for large values of the vortex core energy ϵ_c. We expect α_{xy} to saturate at a finite value in this limit; when all thermally generated vortex fluctuations are suppressed, the remaining field-induced vortices respond to the thermal gradient in a way that is independent of the magnitude of ϵ_c.

Dependence on the number of vortex flavors: Several theories of cuprates predict additional degrees of freedom associated with vortices that endows them with a flavor index.[18,19] Such an extension is readily incorporated in our formalism; the Gauss law is now $\nabla\cdot\boldsymbol{e}=2\pi\Sigma_{\alpha=1}^{N_v}n_{i\alpha}$, where α is the flavor index. Our data show a systematic dependence on the number of internal flavors. We find that both $|M|$ and α_{xy} of single-flavor vortices (solid curves in Fig. 3) are systematically larger than that of vortices with two internal flavors (dotted lines). With multiple vortex species, there is additional configurational entropy associated with the internal degree of freedom. Therefore, the free-energy cost of introducing a vortex into the sample is lower, and the system becomes less diamagnetic. It is more difficult to understand, however, why α_{xy} decreases as the number of species is increased. In phenomenological discussions, the transport coefficient α_{xy} is usually identified with the vortex entropy.[20] Therefore, one may naively expect α_{xy} to increase with the number of internal vortex flavors. Moreover, α_{xy} is equivalent to the vortex thermopower, and if we neglected the logarithmic interactions between vortices, the thermopower is simply the entropy per particle (see below), which increases linearly with the number of internal states associated with such particles. Our numerical results however are in sharp contrast to such expectations. Instead, our results, which have the opposite trend, point toward a scenario that is far more complicated than an ideal gas approximation.

Perhaps the most striking feature of our data is the fact that α_{xy} and $-M/T$ closely track each other. In particular, at high temperatures, our results obey the relation $\alpha_{xy}=-cM/T$, where $c\approx1$, and is difficult to determine accurately due to noise at large temperatures. Recently, it was shown analytically in Ref. 12 that for the 2D *XY* Hamiltonian with overdamped dynamics, $c=1/2$ at high temperatures. Furthermore, one obtains the same relation for Gaussian superconducting fluctuations.[21] Here, we have shown that this relation is even more robust since it hardly depends on the variation in the core energy and the number of distinct vortex species so long as ϵ_c is not much greater than T. This relationship is indicative of a deep underlying principle that seems to hold true over a broad range of parameters.

Discussion: Thus far, we have focused on the Nernst effect due to vortices interacting with a logarithmic Coulomb interaction. As a point of comparison, we now derive the Nernst effect of a noninteracting ideal gas of vortices. For this case, we will show rigorously that α_{xy} is equal to the thermodynamic entropy per vortex. Then, we will introduce interactions through a virial expansion to show the deviations from this result for interacting vortices.

As mentioned above, the transverse thermoelectric conductivity α_{xy} maps under duality to the thermopower of the vortices, i.e., to the dual electric field created by the vortices in response to an applied temperature gradient

$$\alpha_{xy}=\rho_s^0\left.\frac{e_x}{\nabla_x T}\right|_{j=0},$$

where measurement is carried out under open-circuit boundary conditions for the vortices, $\boldsymbol{j}=0$.

Consider noninteracting particles, which can be bosonic, fermionic, or distinguishable (the result will be independent of particle statistics), in a system with Galilean invariance so

that the energy of a particle with momentum k is $\epsilon_k = k^2/2m$. The Boltzmann equation for the particle distribution $g=g(r,k,t)$ is $\dot{r}\cdot\nabla_r g=-(g-g_0)/\tau$, where g_0 is the particle distribution in equilibrium and τ is a relaxation time. In the Boltzmann equation, we have assumed that no external forces are present (however, gradients in chemical potential and temperature are present). Then, the vortex current is

$$\begin{aligned} \boldsymbol{j}(r) &= \int \frac{d^d k}{(2\pi)^d} \boldsymbol{v}_k g(k,r) \\ &= -\frac{2\tau}{md}\nabla_r \left[\int \frac{d^d k}{(2\pi)^d} \frac{k^2}{2m} g(k,r) \right] \\ &= -\frac{2\tau}{md}\nabla_r [\rho_E(r)], \end{aligned}$$

where ρ_E is the energy density of the vortices. Note that, independently of the particle statistics, the energy density of an ideal gas is proportional to the pressure P. Therefore, open-circuit boundary conditions are equivalent to the requirement that the pressure in the system be uniform, $\nabla P=$. Therefore,

$$\alpha_{xy} = -\left.\frac{\partial \mu}{\partial T}\right|_{j=0} = -\left(\frac{\partial \mu}{\partial T}\right)_{P,N} = \left(\frac{\partial S}{\partial N}\right)_{P,T}, \tag{7}$$

where S is the entropy, μ the vortex chemical potential, N the vortex number, and where in the last line we have used a Maxwell relation. Thus, α_{xy} of an ideal gas of vortices is a measurement of entropy per vortex.

Next, we consider the leading correction to α_{xy} due to pairwise interactions among the particles. Assuming that the particles are classical and indistinguishable the interactions can be treated perturbatively with a virial expansion. From the Boltzmann equation above, it is clear that the open-circuit boundary conditions on the particles amount to a constraint of uniform *kinetic energy density*. This in turn implies that instead of holding the pressure constant as in the case of the ideal gas, we must require quantity $P-n^2TB_2(T)$ to remain constant, where B_2 is the second virial coefficient of the system. Therefore,

$$\alpha_{xy} = -\left(\frac{\partial \mu}{\partial T}\right)_{P-n^2TB_2(T),N}. \tag{8}$$

In the dilute limit where the interactions are very weak, i.e., when $B_2 \ll P/(n^2T)$,

$$\alpha_{xy} = \left(\frac{\partial S}{\partial N}\right)_{P,T} - n\frac{\partial}{\partial T}(TB_2). \tag{9}$$

Thus, when $B_2>0$, which is true in the case of repulsive interactions, we see that α_{xy} *decreases* in magnitude and is no longer simply identified with the entropy per particle. Indeed, our numerical calculations strongly suggest that interactions between vortices play an important role in determining the temperature dependence of α_{xy} and invalidate a simple identification of α_{xy} as the vortex transport entropy.

In conclusion, we have presented a method to study the thermodynamic and transport properties of 2D vortex liquids. This method enables us to directly observe the effect of modifying the core energy and the number of vortex species on diamagnetism and Nernst effect. We have found that both quantities persist well above T_{KT} and α_{xy} closely tracks $-M/T$ when $T_{\mathrm{KT}}<T\ll\epsilon_c$. We have provided a detailed analysis of the Nernst effect of a vortex liquid that deals directly with vortex variables. The method presented here can be generalized to study thermal transport of vortex liquids in three dimensions (3D) and can be extended to study quantum phase fluctuations.

We thank P. W. Anderson, S. A. Kivelson, P. A. Lee, and N. P. Ong for very helpful discussions. This work was supported by NSF under Contracts No. DMR-0645691 (A.V.) and No. DMR-0213706 (D.A.H.) and by the Stanford Institute for Theoretical Physics (S.R.).

[1] Y. Wang, L. Li, and N. P. Ong, Phys. Rev. B **73**, 024510 (2006).
[2] V. J. Emery and S. A. Kivelson, Nature (London) **374**, 434 (1995).
[3] J. Corson, R. Mallozzi, J. Orenstein, J. N. Eckstein, and I. Bozovic, Nature (London) **398**, 221 (1999).
[4] L. Miu, D. Miu, G. Jakob, and H. Adrian, Phys. Rev. B **75**, 214504 (2007).
[5] D. S. Fisher, M. P. A. Fisher, and D. A. Huse, Phys. Rev. B **43**, 130 (1991).
[6] L. B. Ioffe and A. J. Millis, Phys. Rev. B **66**, 094513 (2002).
[7] C. Honerkamp and P. A. Lee, Phys. Rev. Lett. **92**, 177002 (2004).
[8] I. Ussishkin, S. L. Sondhi, and D. A. Huse, Phys. Rev. Lett. **89**, 287001 (2002).
[9] S. Mukerjee and D. A. Huse, Phys. Rev. B **70**, 014506 (2004).
[10] S. A. Hartnoll, P. K. Kovtun, M. Müller, and S. Sachdev, Phys. Rev. B **76**, 144502 (2007).
[11] P. W. Anderson, Phys. Rev. Lett. **100**, 215301 (2008).
[12] D. Podolsky, S. Raghu, and A. Vishwanath, Phys. Rev. Lett. **99**, 117004 (2007).
[13] L. Benfatto, C. Castellani, and T. Giamarchi, Phys. Rev. Lett. **98**, 117008 (2007); **99**, 207002 (2007); Phys. Rev. B **77**, 100506(R) (2008).
[14] A. C. Maggs and V. Rossetto, Phys. Rev. Lett. **88**, 196402 (2002); L. Levrel and A. C. Maggs, Phys. Rev. E **72**, 016715 (2005).
[15] D. R. Nelson and J. M. Kosterlitz, Phys. Rev. Lett. **39**, 1201 (1977).
[16] H. Weber and P. Minnhagen, Phys. Rev. B **37**, 5986 (1988).
[17] V. Oganesyan, D. A. Huse, and S. L. Sondhi, Phys. Rev. B **73**, 094503 (2006).
[18] P. A. Lee and X.-G. Wen, Phys. Rev. B **63**, 224517 (2001).
[19] D. P. Arovas, A. J. Berlinsky, C. Kallin, and S.-C. Zhang, Phys. Rev. Lett. **79**, 2871 (1997).
[20] C. Caroli and K. Maki, Phys. Rev. **164**, 591 (1967).
[21] I. Ussishkin (unpublished).